

Evaluation of the biostratigraphy of the Cretaceous-Paleogene boundary interval in the Hendijan oil field, Zagros (SW Iran)

Saeedeh Senemari*

Department of Mining, Faculty of Engineering, Imam Khomeini International University, Qazvin, Iran. Tel: +00982833901126-09127852086
(Fax): + 00982833780073; senemari2004@yahoo.com

Marziyeh Notghi Moghaddam

Department of Geology, Payam-e Noor University, Tehran, I R of Iran; m.n.moghaddam@gmail.com

Manuscript submitted 2nd November, 2016; revised manuscript accepted 29th July, 2017

Abstract The Zagros Basin is part of the Neo-Tethys Basin in Iran and includes three stratigraphic provinces. Exploration studies in this basin are very important due to the presence of large hydrocarbon fields, such as the Hendijan oil field, where The Gurpi and Pabdeh Formations are significant source rocks. This study examines the calcareous nannofossil biostratigraphy of the upper Gurpi Formation and 66m of the Pabdeh Formation in a continuous core taken from a well in the Hendijan oil field, located in southwest Zagros. The 33 genera and 50 species of calcareous nannofossils identified in these samples clearly delineate the Cretaceous/Paleogene boundary in this oil field. In this core, the upper Gurpi Formation spans the upper Lower Maastrichtian to lower Upper Maastrichtian (Zones CC24–25). The overlying Pabdeh Formation is assigned to the terminal Middle Paleocene to Upper Paleocene (Zones NP6–9).

Key words biostratigraphy, calcareous nannofossils, Cretaceous, Paleocene, Paleogene, Hendijan, Zagros

1. Introduction

A thick Phanerozoic sedimentary sequence (Cambrian–Recent) was consistently deposited in a subsiding trough in the Neo-Tethys (Darvishzadeh, 1992). The collision of the Arabian Plate and Central Iranian Block during the Mesozoic and Cenozoic produced the Zagros fold belt, which contains more than 10,000m of post-Paleozoic strata. The fold belt extends NW–SE for about 2000km from SE Turkey through SW Iran (Motiei, 1995; Alavi, 2004; Kamali *et al.*, 2006) and is one of the largest known oil fields. It has been referred to as the “Agreement Area” since 1954. The Gurpi Formation (Fm) and Pabdeh Fm are exposed throughout most of the Agreement Area in southwestern Iran; both formations are present in all three provinces (Khuzestan, Lurestan and Fars) in the Zagros fold belt (Kamali *et al.*, 2006). The name, Gurpi, derives from the Kuh e-Gurpi in Khuzestan Province, and its type section in North Lali oil field (NE Masjed Soleiman) is comprised of argillaceous limestones with shales and gray marls. In North Lali oilfield, the Gurpi Fm overlies the Ilam Fm and is disconformably overlain by the Pabdeh Fm. The name of the Pabdeh Fm is derived from Kuh e-Pabdeh in Khuzestan Province, where James & Wynd (1965) described the type section at Tang e-Pabdeh in North Lali oilfield, which consisted of shales and argillaceous limestones with marls. The lithologies of the Gurpi and Pabdeh Fms are very similar, making their distinction in the field nearly impossible and microscopic studies (e.g., calcareous nannofossils) a necessity. These

formations have previously been investigated by various aspects of paleontology (e.g., Mohseni & Al-Aasm, 2004; Khosrowtehrani, 2008; Bahrami, 2009; Behbahani *et al.*, 2010). The calcareous nannofossil biostratigraphy of various formations in the Zagros Basin have also been studied in recent years (e.g., Hadavi *et al.*, 2007; Senemari & Sohrabi Molla Usefi, 2013). The current study is the first to detail calcareous nannofossil assemblages across the Cretaceous/Paleogene (K/Pg) boundary interval in the Hendijan oilfield. The main purpose of our research is to establish correlations to global biozonations and evaluate paleoecologic conditions for the study area.

2. Material and methods

The Hendijan oilfield is located in the northwestern Persian Gulf on Dezful Embayment. The sequence considered is located in the SE Dezful Embayment, about 170km southeast of Ahwaz, between 49.5–50°E longitude and 30–30.75°N latitude (Figure 1). Sediments of the upper Gurpi and Pabdeh Fms were selected to investigate the K/Pg boundary interval using calcareous nannofossils. The studied section is an 80m continuous core that consists mainly of shales, marls and shaley limestones. Lithologies (argillaceous limestone, shale and marl) transitional between the Pabdeh Fm and the overlying Jahrum Fm are present near the top of the core. Seventy-eight samples were collected systematically in intervals between 50–100cm throughout the Gurpi and Pabdeh Fms. Only one sample was taken from the overlying Jahrum Fm.

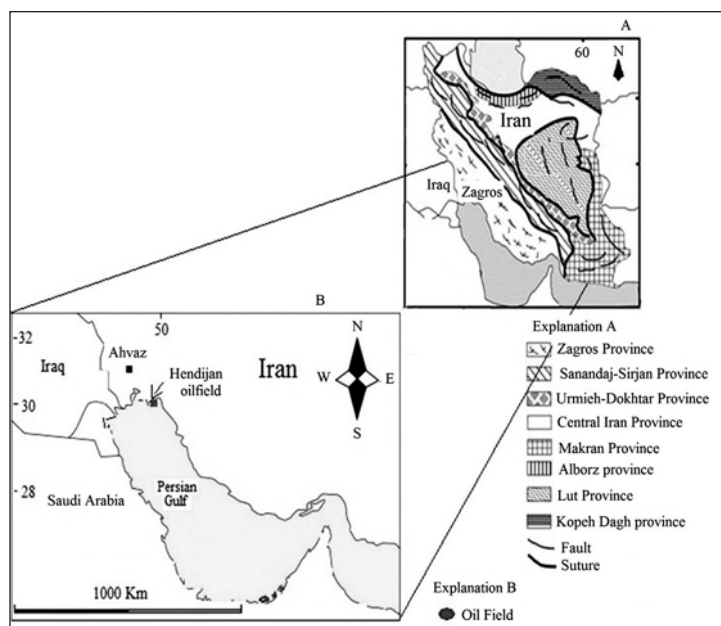


Figure 1: A: Generalized map of Iran showing eight geologic provinces, adapted from Heydari *et al.* (2003); B: Locality map of the studied area, Hendijan oil field

Samples were prepared by the standard smear slide method (Bown & Young, 1998) directly from raw samples and rock fragments without centrifuging. All slides were studied under cross polarized light (XPL) and phase contrast (PC) at a magnification of 1000X using an Olympus microscope.

Calcareous nannofossil taxonomic concepts followed Perch-Nielsen (1985a, b) and Bown (1998). Nannofossil assemblages represent counts of the first 100 fields of view (FOV) and are presented in Table 1 as follows: R = rare (1 specimen per 11–100FOV); F = few (1 specimen per 2–10FOV); C = common (1–10 specimens per FOV); A = abundant (>10 specimens per FOV). At least 300 specimens were counted in each sample for paleoecologic and biostratigraphic discussion. To avoid enlarging Table 1, each row in Table 1 represents three samples.

3. Biostratigraphy

Results from studied samples show the nannofossil biostratigraphy of the upper Gurpi and Pabdeh Fms relative to the K/Pg boundary (Table 1). A total of 17 genera and 27 species were identified in samples from the Gurpi Fm, while 17 genera and 24 species were identified from samples in the Pabdeh Fm and the base of the overlying “Transitional Zone” to the Jahrum Fm. A major disconformity separating the “mid” Maastrichtian Gurpi Fm and Upper Paleocene Pabdeh Fm has been linked to epeirogenic movements in the Zagros fold belt (James & Wynd, 1965; Motiei, 1994). We estimate the disconformity identified in the core encompasses about nine million years, using the time scale of Gradstein *et al.*, (2012).

We apply the CC zonation of Sissingh (1977, 1978) for the Cretaceous Gurpi Fm, whereas both the NP zones

of Martini (1971) and CP zones of Okada & Bukry (1980) are applied to the Paleogene Pabdeh Fm. Other main references are used (Perch-Nielsen, 1985a, b; Burnett, 1998; Self-Trail, 2001) for Maastrichtian to Paleocene nannofossil biostratigraphy and their calibration to the Geologic time scale of Gradstein *et al.*, (2012). Abbreviations used herein are FO for the first occurrence and LO for the last occurrence. Several of the species identified in this study are illustrated in Plates 1–2.

3.1 Biozonation of the upper Gurpi Formation

The *Reinhardtites levis* (CC24) and *Arkhangelskiella cymbiformis* (CC25) Zones have been identified in samples from the Gurpi Fm (Table 1). The total thickness of the biozones CC24 (6m) and CC25 (9m) is 15m. The LO of *R. levis* marks the boundary between these two zones and is a rough approximation for the top of the Lower Maastrichtian (see Gradstein *et al.*, 2012). The base of *Micula praemurus* was observed in the same core sample as the highest occurrence of *R. levis*. Self-Trail (2001) placed the FO of *M. praemurus* near the base of Subzone CC25a. The core is thought no older than Zone CC24 because of the absence of *Tranolithus orionatus* (= *T. phacelosus*), whose extinction marks the top of Zone CC23. *Lithraphidites quadratus* and *Micula murus* were both observed in the highest sample from the Gurpi Fm. The FOs of these two species have been utilized as the base of Subzones CC25b/c by various authors (Sissingh, 1978; Perch-Nielsen, 1985a, Self-Trail, 2001). *Micula praemurus* was also observed in this top sample. Self-Trail (2001) reported the LO of this species within Subzone CC26a. The absence of *Micula prinsii*, which marks the base of

Formation	Lithology of core	Period	Epoch	Stage	Biozonation	Zonation Okada & Bukry, 1980	This study	Sample no.	Depth (m)	Calcareous nanofossils of Late Cretaceous	Calcareous nanofossils of Paleocene/Thanetian
Gurpi		Cretaceous	Late	Maastrichtian	NP10	CC25	NP10	78	2929	<i>Arhangelskella cymbiformis</i> <i>Arhangelskella sp.</i> <i>Calculus obscurus</i> <i>Cerrolithoides aculeus</i> <i>Chastozygus amphiporus</i> <i>Egglethius gorkae</i> <i>Egglethius hursseithi</i> <i>Lithraphidites carnioleus</i> <i>Lithraphidites quadratus</i> <i>Lacunarhabdulus covei</i> <i>Microrhabdulus belgicus</i> <i>Microrhabdulus decoratus</i> <i>Micula decussata</i> <i>Micula concava</i> <i>Micula murus</i> <i>Micula praemurus</i> <i>Prediscosphaera cretacea</i> <i>Quadratum gothicum</i> <i>Rhagodiscus angustus</i> <i>Reinhardtites levis</i> <i>Micula cubiformis</i> <i>Tetrapodorbabulus decorus</i> <i>Thoracosphaera operculata</i> <i>Watanabea barnesae</i> <i>Watanabea bipora</i> <i>Braarudosphaera bigelowii</i> <i>Biantholobites sparsus</i> <i>Cratichnoidites tenuis</i> <i>Chiasmoidites consuetus</i> <i>Chiasmoidites bideus</i> <i>Ericsoma subperthae</i> <i>Discoaster araneus</i> <i>Discoaster mohleri</i> <i>Discoaster multiradiatus</i> <i>Heliosolithus maclellis</i> <i>Ericsoma robusta</i> <i>Fasciculolithus bilyanae</i> <i>Heliosolithus kleinpellii</i> <i>Heliosolithus cantabrigiae</i> <i>Markabius inversus</i> <i>Neococcolithes protenus</i> <i>Prinsius bisulcus</i> <i>Prinsius marshalli</i> <i>Placozygus sigmoides</i> <i>Rhomboaster cuspid</i> <i>Sphenolithus antrypopus</i> <i>Sphenolithus primus</i> <i>Tribrachiatulus bramlettei</i>	
Pabdeh		Tertiary / Paleogene	Paleocene / Late Paleocene	Thanetian	NP8	NP8	NP8	52	2895	<i>Arhangelskella cymbiformis</i> <i>Arhangelskella sp.</i> <i>Calculus obscurus</i> <i>Cerrolithoides aculeus</i> <i>Chastozygus amphiporus</i> <i>Egglethius gorkae</i> <i>Egglethius hursseithi</i> <i>Lithraphidites carnioleus</i> <i>Lithraphidites quadratus</i> <i>Lacunarhabdulus covei</i> <i>Microrhabdulus belgicus</i> <i>Microrhabdulus decoratus</i> <i>Micula decussata</i> <i>Micula concava</i> <i>Micula murus</i> <i>Micula praemurus</i> <i>Prediscosphaera cretacea</i> <i>Quadratum gothicum</i> <i>Rhagodiscus angustus</i> <i>Reinhardtites levis</i> <i>Micula cubiformis</i> <i>Tetrapodorbabulus decorus</i> <i>Thoracosphaera operculata</i> <i>Watanabea barnesae</i> <i>Watanabea bipora</i> <i>Braarudosphaera bigelowii</i> <i>Biantholobites sparsus</i> <i>Cratichnoidites tenuis</i> <i>Chiasmoidites consuetus</i> <i>Chiasmoidites bideus</i> <i>Ericsoma subperthae</i> <i>Discoaster araneus</i> <i>Discoaster mohleri</i> <i>Discoaster multiradiatus</i> <i>Heliosolithus maclellis</i> <i>Ericsoma robusta</i> <i>Fasciculolithus bilyanae</i> <i>Heliosolithus kleinpellii</i> <i>Heliosolithus cantabrigiae</i> <i>Markabius inversus</i> <i>Neococcolithes protenus</i> <i>Prinsius bisulcus</i> <i>Prinsius marshalli</i> <i>Placozygus sigmoides</i> <i>Rhomboaster cuspid</i> <i>Sphenolithus antrypopus</i> <i>Sphenolithus primus</i> <i>Tribrachiatulus bramlettei</i>	
Gurpi		Cretaceous	Late	Maastrichtian	NP10	CC25	NP10	78	2929	<i>Arhangelskella cymbiformis</i> <i>Arhangelskella sp.</i> <i>Calculus obscurus</i> <i>Cerrolithoides aculeus</i> <i>Chastozygus amphiporus</i> <i>Egglethius gorkae</i> <i>Egglethius hursseithi</i> <i>Lithraphidites carnioleus</i> <i>Lithraphidites quadratus</i> <i>Lacunarhabdulus covei</i> <i>Microrhabdulus belgicus</i> <i>Microrhabdulus decoratus</i> <i>Micula decussata</i> <i>Micula concava</i> <i>Micula murus</i> <i>Micula praemurus</i> <i>Prediscosphaera cretacea</i> <i>Quadratum gothicum</i> <i>Rhagodiscus angustus</i> <i>Reinhardtites levis</i> <i>Micula cubiformis</i> <i>Tetrapodorbabulus decorus</i> <i>Thoracosphaera operculata</i> <i>Watanabea barnesae</i> <i>Watanabea bipora</i> <i>Braarudosphaera bigelowii</i> <i>Biantholobites sparsus</i> <i>Cratichnoidites tenuis</i> <i>Chiasmoidites consuetus</i> <i>Chiasmoidites bideus</i> <i>Ericsoma subperthae</i> <i>Discoaster araneus</i> <i>Discoaster mohleri</i> <i>Discoaster multiradiatus</i> <i>Heliosolithus maclellis</i> <i>Ericsoma robusta</i> <i>Fasciculolithus bilyanae</i> <i>Heliosolithus kleinpellii</i> <i>Heliosolithus cantabrigiae</i> <i>Markabius inversus</i> <i>Neococcolithes protenus</i> <i>Prinsius bisulcus</i> <i>Prinsius marshalli</i> <i>Placozygus sigmoides</i> <i>Rhomboaster cuspid</i> <i>Sphenolithus antrypopus</i> <i>Sphenolithus primus</i> <i>Tribrachiatulus bramlettei</i>	

Table 1: Stratigraphic chart of Gurpi and Pabdeh Formations based on Calcareous Nannofossils, Hendijan oil field located Southwestern Zagros. *Braarudosphaera bigelowii* is identified in both Fms. Species abundance: R = rare (1 specimen per field of view [FOV] 11–100), F = few (1 specimen per 2–10FOV), C = common (1–10 specimen per FOV), A = abundant (>10 specimen per FOV)

Subzone CC26b (Self-Trail, 2001), is further evidence that the terminal Maastrichtian is absent in the core.

3.2 Biozonation of the Pabdeh Formation

The following succession of biozones was recognized in the Pabdeh Fm: *Heliolithus kleinpellii* Zone (NP6/CP5), *Discoaster mohleri* Zone (NP7/CP6), *Heliolithus riedelii* (NP8)/*Discoaster nobilis* (CP7) Zone, and *Discoaster multiradiatus* Zone (NP9/CP8). The total thickness of the Paleocene biozones NP6 (19m), NP7 (14m), NP8 (12m) and NP9 (20m) is 65m. The single sample from the overlying "Transitional Zone" contains *Tribrachiatus bramlettei*, which marks the base of the *T. contortus* Zone (NP10/CP9) and approximates the base of the Eocene. The lowest sample in the Pabdeh Fm contains *H. kleinpellii*, the FO of which marks the base of Zone NP6 (CP5). *Sphenolithus anarrhopus* is also present in this sample. The FO of this species was placed in mid-Zone NP6 by Perch-Nielsen (1985b). The FO of *D. mohleri* marks the base of Zone NP7 (CP6) and is observed in the next sample up section. The base of Zone NP8 (NP7) is approximated by the lowest occurrence of *D. araneus* in the core (Table 1). The base of Zone NP9 (CP8) is identified by the base of the marker species, *D. multiradiatus*. Three other events are coincident with the base of *D. multiradiatus* in the core: the bases of *F. lillianae* and *R. cuspidis*, and the top of *H. kleinpellii*.

4. Paleoecology

Recovered nannofossil assemblages are indicative of open marine conditions and a deep marine environment (Okada & Bukry, 1980; Wise, 1988; Chira & Igritan, 2004; Lees *et al.*, 2004; Thierstein & Young, 2004; Dunkley Jones *et al.*, 2008). Several have low-latitude (i.e. warm water) affinities, such as *Discoaster*, *Ericsonia*, *Fasciculithus* and *Sphenolithus* (Bralower, 2002; Gibbs *et al.*, 2006; Self-Trail *et al.*, 2012; Villa *et al.*, 2008). Also of significance are common *B. bigelowii* in the bottom two samples of the Pabdeh Fm, which could indicate nutrient enrichment and/or eutrophic environments (Konno *et al.*, 2007) for Zones NP6-NP7. In the Cretaceous, high abundances of certain taxa (*A. cymbiformis*, *Watznaueria barnesiae*, *Eiffellithus turriseiffelii* and *Ceratolithoides aculeus*) could be evidence for oligotrophic surface waters (Thierstein, 1976; Watkins *et al.*, 1996; Lees, 2002; Herrle, 2003; Bown *et al.*, 2004; Kaya Ozer, 2014; Linnert & Mutterlose, 2009; Thibault & Gardin, 2010); however, this abundance may also be explained by poor preservation.

5. Conclusion

In this study, 33 genera and 50 species of calcareous nannofossil have been identified in a detailed study of an 80m core from a well in the Hendijan oilfield. Six calcareous nannofossil zones have been recognized in the Gurpi and Pabdeh Fms present in this core. As expected, calcareous nannofossil assemblages show a significant change across the K/Pg boundary. This change is exaggerated by a major

disconformity between the two formations, where the early Late Maastrichtian (CC25) Gurpi Fm is overlain by the latest Middle Paleocene (mid-Zone NP6) Pabdeh Fm, giving a disconformity of ~9My.

Acknowledgements

The authors would like to thank both manuscript reviewers and Dr. Jamie Shamrock for her comments that helped improve the manuscript.

References

- Alavi, M. 2004. Regional stratigraphy of the Zagros fold-thrust belt of Iran and its proforeland evolution. *American Journal of Science*, **304**: 1–20.
- Bahrami, M. 2009. Microfacies and sedimentary environments of Gurpi and Pabdeh Formations in Southwest of Iran. *American Journal of Applied Science*, **6**(7): 1295–1300.
- Behbahani, R., Mohseni, H., Khodabakhsh, S. & Atashmard, Z. 2010. Depositional environment of the Pabdeh Formation (Paleogene) elucidated from trace fossils, Zagros Basin, W Iran. *1st International Applied Geological Congress*, Iran: 1004–1007.
- Bown, P. (Ed.) 1998. *Calcareous Nannofossil Biostratigraphy*. British Micropaleontological Society Publication Series. Academic Publishers, Dordrecht, Boston, London: 328pp.
- Bown, P.R. & Young, J.R. 1998. Techniques. In: P.R. Bown (Ed.). *Calcareous Nannofossil Biostratigraphy*. Academic Publishers, Dordrecht, Boston, London: 16–28.
- Bown, P.R., Lees, J.A. & Young, J.R. 2004. Calcareous nannoplankton evolution and diversity through time. In: H.R. Thierstein & J.R. Young, (Eds). *Coccolithophores: From Molecular Processes to Global Impact*. Springer Verlag: 481–508.
- Bralower, T.J. 2002. Evidence of surface water oligotrophy during the Paleocene-Eocene thermal maximum: Nannofossil assemblage data from Ocean Drilling Program Site 690, Maud Rise, Weddell Sea. *Paleoceanography*, **17**(2): 1–12.
- Burnett, J.A. 1998. Upper Cretaceous. In: P.R. Bown (Ed.). *Calcareous Nannofossil Biostratigraphy*. Chapman and Hall, London: 132–199.
- Chira, C. & Igritan, A. 2004. Eocene Oligocene calcareous nannofossils from Hiedin area, between Hodis and Tetis (Transylvania, Romania): biostratigraphy and paleoecological data. *Studia UBB. Geologia*, **49**(2): 109–127.
- Darvishzadeh, A. 1992. *Geology of Iran*. Amir kabir Publication Company, Tehran: 625pp.
- Dunkley Jones, T., Bown, P.R., Pearson, P.N., Wade, B.S., Coxall, H.K. & Lear, C.H. 2008. Major shifts in calcareous phytoplankton assemblages through the Eocene-Oligocene transition of Tanzania and their implications for low-latitude primary production. *Paleoceanography*, **23**(4): PA4204.
- Gibbs, S.J., Bralower, T.J., Bown, P.R., Zachos, J.C. & Bybell, L.M. 2006. Shelf and open-ocean calcareous phytoplankton assemblages across the Paleocene-Eocene thermal maximum: implications for global productivity gradients. *Geology*, **34**(3): 233–236.

- Gradstein, F.M., Ogg J.G., Schmitz, M.D. & Ogg, G.M. 2012. *The Geologic Time Scale 2012*, Volume 2. Elsevier, 1144pp.
- Hadavi, F., Khosrowtehrani, K. & Senemari, S. 2007. Biostratigraphy of calcareous nannofossils of Gurpi Formation in North Gachsaran. *Iranian Journal of Geology*, **64**: 14–23.
- Herrle, J.O. 2003. Reconstructing nutricline dynamics of mid-Cretaceous oceans: evidence from calcareous nannofossils from the Niveau Paquier black shale (SE France). *Marine Micropaleontology*, **47**: 307–321.
- Heydari, E., Hassanzadeh, J., Wade, W.J. & Ghazi, A.M. 2003. Permian-Triassic boundary interval in the Abadeh section of Iran with implications for mass extinction, part 1, sedimentology. *Palaeogeography, Palaeoclimatology, Palaeoecology*, **193**: 405–423.
- James, G.A. & Wynd, J.G. 1965. Stratigraphic nomenclature of Iranian oil consortium, agreement area. *American Association of Petroleum Geologists Bulletin*, **49**(12): 2182–2245.
- Kamali, M.R., Fathi Mobarakabad, A. & Mohsenian, E. 2006. Petroleum Geochemistry and Thermal Modeling of Pabdeh Formation in Dezful Embayment. *Journal Science of University Tehran*, **32**(2): 1–11.
- Kaya Ozer, C. 2014. Calcareous nannofossil assemblage changes and stable isotope data from Maastrichtian to Selandian in the Akveren Formation, Western Black Sea, Turkey. *Arabian Journal of Geosciences*, **7**: 1233–1247.
- Khosrowtehrani, Kh. 2008. *Applied Micropaleontology*. Tehran University Press, Iran, Tehran: 432pp.
- Konno, S., Harada, N., Narita, H. & Jordan, R.W. 2007. Living *Braarudosphaera bigelowii* (Gran and Braarud) Deflandre in the Bering Sea. *Journal of Nannoplankton Research*, **29**(2): 78–87.
- Lees, J.A., 2002. Calcareous nannofossil biogeography illustrates palaeoclimate change in the Late Cretaceous Indian Ocean. *Cretaceous Research*, **23**: 537–634.
- Lees, J.A., Bralower, T.J., Herbert, T., Bergen, J.A., Self-Trail, J. & de Romero, L. 2004. Towards a high-resolution chronostratigraphy for the upper Cretaceous. *Journal of Nannoplankton Research*, 10th Conference of the International Nannoplankton Association, Abstracts, Lisbon, Portugal, **26**(2):71.
- Linnert, C., & Mutterlose, J., 2009. Evidence of increasing surface water oligotrophy during the Campanian- Maastrichtian boundary interval: Calcareous nannofossils from DSDP Hole 390A (Black Nose). *Marine Micropaleontology*, **73**: 26–36.
- Martini, E. 1971. Standard Tertiary and Quaternary Calcareous Nannoplankton Zonation. In: A. Farinacci (Ed.). *Proceedings of the Second Planktonic Conference Roma 1970*. Edizioni Tecnoscienza, Rome, **2**: 739–785.
- Mohseni, H. & Al-Aasm, I.S. 2004. Tempestite deposits on a storm-influenced carbonate ramp: an example from the Pabdeh Formation (Paleogene), Zagros Basin, SW Iran. *Journal of Petroleum Geology*, **27**(2): 163–178.
- Motiei, H. 1994. *Geology of Iran: Stratigraphy of Zagros*. Geological Survey of Iran, Tehran: 536pp.
- Motiei, H. 1995. *Petroleum Geology of Zagros*. Geological Survey of Iran, Tehran: 589pp.
- Okada, H. & Bukry, D. 1980. Supplementary modification and introduction of code numbers to the low-latitude coccolith biostratigraphic zonation (Bukry, 1973; 1975). *Marine Micropaleontology*, **5**: 321–325.
- Perch-Nielsen, K. 1985a. Mesozoic Calcareous Nannofossils. In: H.M. Bolli, J.B. Saunders & K. Perch-Nielsen (Eds). *Plankton Stratigraphy*. Cambridge University Press, Cambridge: 329–426.
- Perch-Nielsen, K. 1985b. Cenozoic Calcareous Nannofossils. In: H.M. Bolli, J.B. Saunders & K. Perch-Nielsen (Eds). *Plankton Stratigraphy*. Cambridge University Press, Cambridge: 427–554.
- Self-Trail, J.M. 2001. Biostratigraphic subdivision and correlation of upper Maastrichtian sediments from the Atlantic Coastal Plain and Blake Nose, western Atlantic. In: D. Kroon, R.D. Norris & A. Klaus (Eds). *Western North Atlantic Paleogene and Cretaceous Paleooceanography*, Geological Society, London, Special Publications, **183**: 93–110.
- Self-Trail, J.M., Powars, D.S., Watkins, D.K. & Wandless, G.A. 2012. Calcareous nannofossil assemblage changes across the Paleocene–Eocene Thermal Maximum: Evidence from a shelf setting. *Marine Micropaleontology*, **92–93**: 61–80.
- Senemari, S. & Sohrabi Molla Usefi, M. 2013. Evaluation of Cretaceous–Paleogene boundary based on calcareous nannofossils in section of Pol Dokhtar, Lorestan, southwestern Iran. *Arabian Journal of Geosciences*, **6**: 3615–3621.
- Sissingh, W. 1977. Biostratigraphy of Cretaceous calcareous nannoplankton. *Geologie en Mijnbouw*, **56**: 37–65.
- Sissingh, W. 1978. Microfossil biostratigraphy and stage-stratotypes of the Cretaceous. *Geologie en Mijnbouw*, **57**(3): 433–440.
- Thibault, N. & Gardin, S. 2010. The calcareous nannofossil response to the end-Cretaceous warm event in the Tropical Pacific. *Palaeogeography, Palaeoclimatology, Palaeoecology*, **291**: 239–252.
- Thierstein, H.R. 1976. Mesozoic calcareous nannoplankton. *Micropaleontology*, **1**: 325–362.
- Thierstein, H.R. & Young, J.R. 2004. *Coccolithophores: From Molecular Processes to Global Impact*. Springer: 565pp.
- Villa, G., Fioroni, C., Pea, L., Bohaty, S. & Persico, D. 2008. Middle Eocene-late Oligocene climate variability: Calcareous nannofossil response at Kerguelen Plateau, Site 748. *Marine Micropaleontology*, **69**: 173–192.
- Watkins, D.K., Wise, S.W. Pospichal, J.J. & Crux, J. 1996. Upper Cretaceous calcareous nannofossil biostratigraphy and paleoecology of the southern ocean. In: A. Moguilevsky & R. Whatley (Eds). *Microfossils and Oceanic Environments*. University of Wales, Aberystwyth Press, Wales: 355–381.
- Wise, S.W. 1988. Mesozoic and Cenozoic history of calcareous nannofossils in the region of the Southern Ocean. *Palaeogeography, Palaeoclimatology, Palaeoecology*, **76**:157–179.

Plate 1

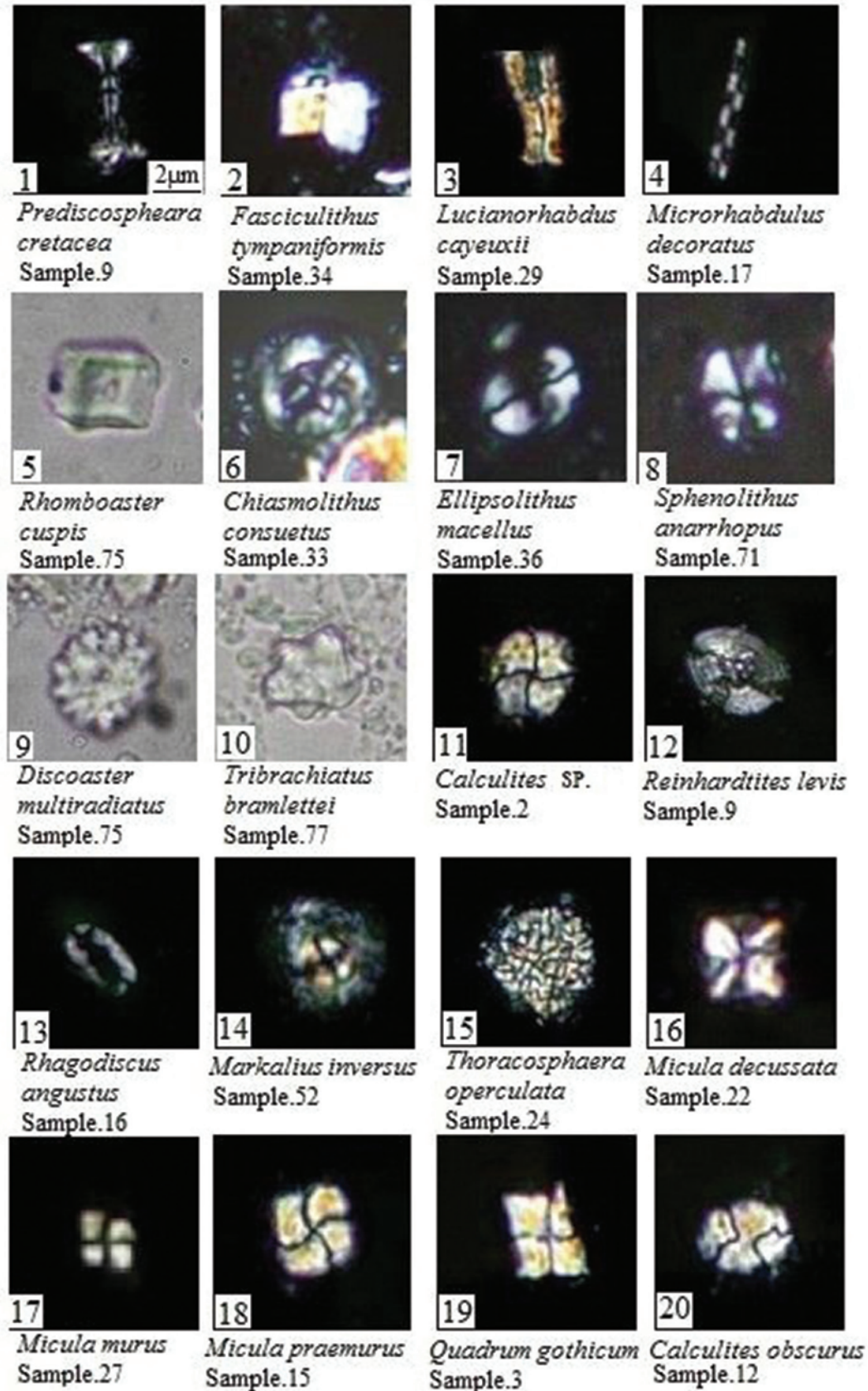


Plate 1: All figures in XPL except figures 5, 9, 10 in PPL, light micrographs $\times 2500$

Plate 2

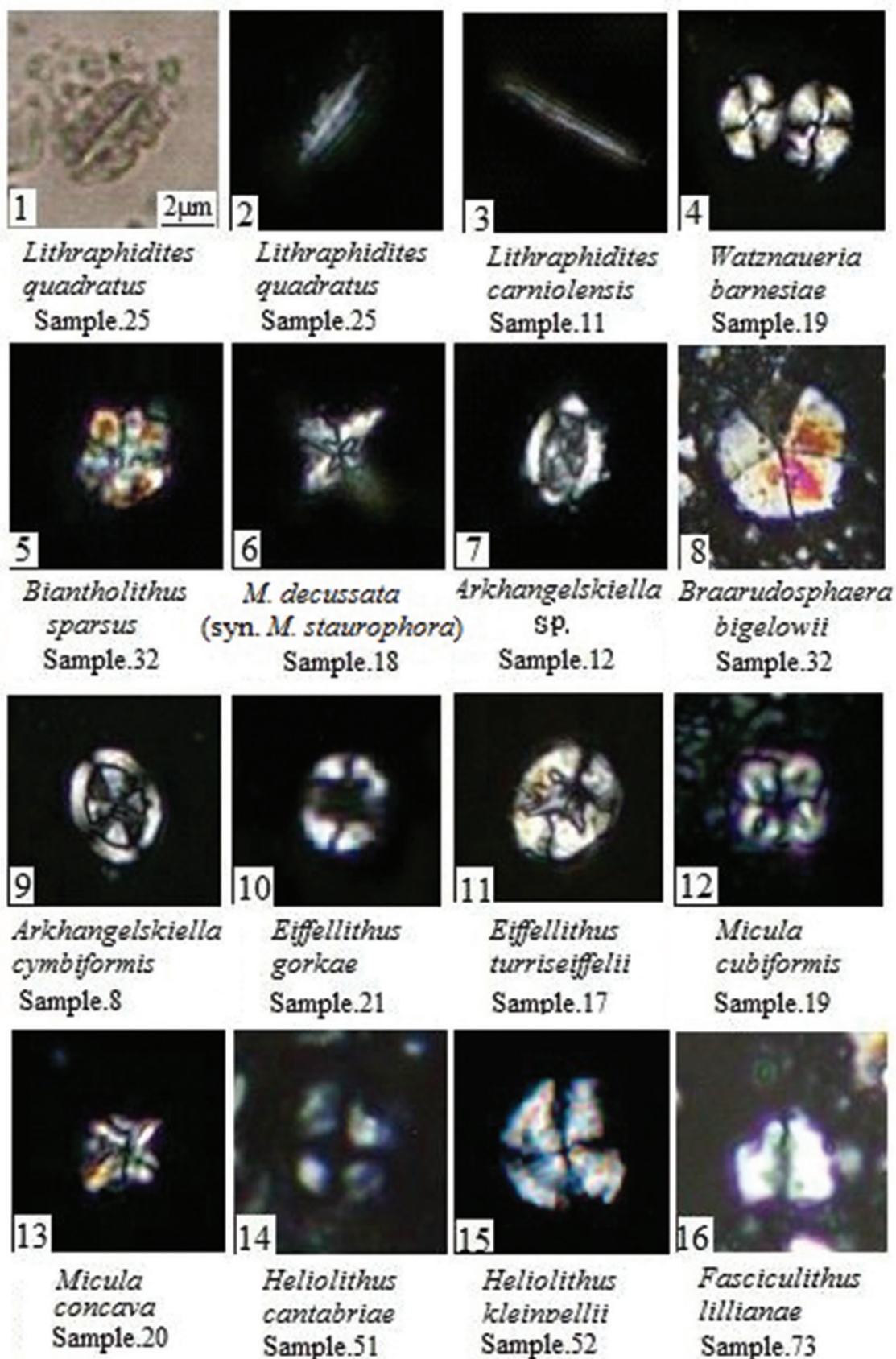


Plate 2: All figures in XPL except figure 1 in PPL, light micrographs $\times 2500$